Biochem. J. (1987) 245, 821–829 (Printed in Great Britain)



# The role of aromatic side chain residues in micelle binding by pancreatic colipase

## Fluorescence studies of the porcine and equine proteins

Jonathan C. McINTYRE, Patricia HUNDLEY and W. David BEHNKE
Department of Biochemistry and Molecular Biology, University of Cincinnati College of Medicine, Cincinnati, OH 45267, U.S.A.

Fluorescence techniques have been employed to study the interaction of porcine and equine colipase with pure taurodeoxycholate and mixed micelles. Nitrotyrosine-55 of porcine colipase is obtained by modification with tetranitromethane (low excess, in the presence of taurodeoxycholate) of the protein followed by gel filtration and ion-exchange chromatography. Verification of the residue modified was obtained by h.p.l.c. peptide purification and sequence analysis. Reduction and quantitative reaction with dansyl chloride yields a fluorescent derivative that is twice as active in conjunction with lipase as is native colipase and that exhibits a strong emission band at 550 nm. Addition of micellar concentrations of taurodeoxycholate causes a 4.3-fold increase in the emission maximum as well as a 70 nm blue shift to 480 nm. Inclusion of oleic acid to form a mixed micelle reduces these spectral effects. Scatchard analysis of the data yield a $K_d$ of $6.8 \times 10^{-4}$ M and a single colipase-binding site for taurodeoxycholate micelles. The data, by analogy to a phospholipase system, are consistent with a direct insertion of dansyl-NH-tyrosine-55 into the micelle. The presence of a single tryptophan residue (Trp-52) in equine colipase provides an intrinsic fluorescent probe for studying protein–micelle interaction. The emission maximum of horse colipase at 345 nm indicates a solvent-accessible tryptophan residue which becomes less so on binding of micelles. A blue shift of 8 nm and a 2-fold increase in amplitude is indicative of a more hydrophobic environment for tryptophan induced by taurodeoxycholate micelles. There is also a decrease in $K_{SV}$ for acrylamide quenching in the presence of micelles, which further supports a loss of solvent accessibility. The most dramatic pH effects are observed with KI quenching, and may indicate the presence of negative charges near Trp-52.

## INTRODUCTION

Colipase is a small secretory protein cofactor from the exocrine pancreas which plays an essential role in the conversion of dietary triacylglycerols into monoacylglycerols and fatty acids in the duodenum and upper jejunum [1,2]. Colipase reverses the inhibitory effects of bile salts, which at physiological concentrations hinder the binding of pancreatic lipase (EC 3.1.1.3) to the interface of water-insoluble triacylglycerol substrates [3] and serves as an anchor for the lipase to the mixed interface [2,3]. As a consequence of this interaction, lipase is protected against surface denaturation. These interactions require the presence of at least two essential surface sites of colipase, one for recognition of the interface and a second for lipase binding. The exact chemical nature of these sites as well as their topographical locations have remained unknown and as such are the subject of continued interest and speculation.

Small-angle neutron scattering studies [4] have shown that bile salt monomers are not dispersed over the entire surface of colipase in the complex, but in fact form micelle clusters distinct from and in juxtaposition to the protein molecule. From c.d. studies using chemical modification techniques and generation of extrinsic Cotton effects [5,6], spectral perturbations of modified tyrosyl residues only occur at concentrations at which taurodeoxycholate forms micelles (critical micelle concentration of approx. 1 mM). This, therefore, strongly supports the theory that colipase possesses a well-defined and unique detergent-binding site which is also presumed to be the interface recognition site of the cofactor.

Porcine [7] and equine [8] colipases both contain three tyrosyl residues at positions 55, 58 and 59, forming a hydrophobic (and possible hydrogen-bonding) cluster region between two disulphide bridges that has been designated as the 'tyrosine loop' region [6]. Conformation analyses of colipase have been performed using a variety of biophysical techniques, including u.v. spectroscopy, c.d. and n.m.r. techniques, the latter indicating that one of the 'loop' tyrosyl residues is restricted in its motion [9–11]. Photo-chemically induced dynamic nuclear polarization studies indicated that one of these tyrosyl residues is also inaccessible to excited flavin dye molecules [12,13]. Thus, if these can be presumed to be the same residue, a tyrosine is 'buried' in colipase while the other two residues were shown by the same techniques to be accessible, therefore possibly forming at least part of the binding domain for bile salts.

Differential u.v. spectroscopy [14–17] and spectrofluorometry [17] have supported some of the aforementioned conclusions, the former indicating a strong u.v. perturbation of two tyrosyl residues consistent with the transfer of these intrinsic chromophores into a hydrophobic interior region of an interacting micelle. Rather surprisingly, no direct interaction has been seen using tyrosine fluorescence [17].

Aromatic residues have been reported to be involved in pancreatic phospholipase $A_2$–interface interaction [18]. Nitrated phospholipase $A_2$ derivatives possessing

nitrotyrosine were purified and evidence was obtained that Tyr-19 and Tyr-69 are involved in micelle binding [19], a conclusion at least partially consistent with X-ray crystallographic studies on the bovine enzyme, which indicated that Tyr-69 is part of the domain of interface recognition [20,21] as is Leu-19, which is a tyrosine in the horse enzyme. Horse [dansyl-NH-Tyr$^{19}$]phospholipase exhibits a 400% increase in dansyl fluorescence and a 27 nm blue shift from 515 to 488 nm, and increases the binding ($K_d$) from 0.5 to 0.27 nM [19]. It is likely that steric constraints are relaxed in the phospholipase (and colipase) micelle system such that even the presence of a bulky group will not compromise binding.

The precise role of tyrosyl residues in colipase with regard to micelle interaction is as yet not completely understood, particularly since nitration (and other modifications) does not apparently affect the ability of colipase to activate lipase in a triacylglycerol/bile salt system [22], a result confirmed in our laboratory. It was found, however, that the p$K_a$ of the nitrotyrosine residues in nitrated colipase is the same as that of free nitrotyrosine (p$K$ 6.8) [5], but is shifted to 7.6 in the presence of taurodeoxycholate micelles [6]. This upward shift in p$K$ may explain why nitrated colipase can reactivate lipase in a triacylglcyerol/taurodeoxycholate system at pH 7.5 [6]. One of the purposes of the present paper is to elucidate further the role of tyrosyl residue(s) in colipase using specific chemical modification and substitution of a fluorophore in order to employ high resolution fluorometric techniques to study micelle interactions.

Equine isocolipases possess a tryptophan residue at position 52 instead of a phenylalanine in the pig protein and a lysine in the human [23]. This provides an opportunity to study the specific contribution of this residue to the intrinsic fluorescence of the protein, since this is the only tryptophan present in the molecule. It will also allow study of the environment of this residue in the presence of bile salts and the effects of this interaction on the quenching of tryptophan by acrylamide, iodide and caesium ions.

## MATERIALS AND METHODS

### Materials

Porcine pancreatic lipase was kindly provided by Dr. M. Rovery and her colleagues in Marseille.

Both equine and porcine colipases were isolated according to the procedure of Chapus *et al.* [24], initially using a commercial source of pancreatic powder (Sigma). With this particular source, the isolated porcine colipase still bound considerable amounts of lipid material, which on several occasions obscured amino acid composition data. With acetone powder prepared from fresh porcine pancreas (Kahns) in our laboratory, the results of chemical modification were exactly as those reported by DeCaro *et al.* [6]. Such difficulties were not encountered with the equine system.

Tetranitromethane was purchased from Aldrich Chemical Co. and was extracted with quartz-distilled water (5X) prior to use. Sodium taurodeoxycholate and dansyl chloride were purchased from Sigma; the former was recrystallized from ethanol according to Sari *et al.* [17]. DE-32 cellulose was purchased from Whatman, while Sephadex G-25 and G-50 were obtained from Pharmacia. Acrylamide was purchased from Bio-Rad and recrystallized from ethanol/water. Caesium chloride (99.95% purity) was purchased from the Var Lac Oid Chem. Co. Inc., Bergenfield, NJ, U.S.A. All other reagents were of the highest quality available from standard sources.

### Methods

Spectrofluorometric measurements were made using a Perkin–Elmer MPF-44A spectrofluorometer equipped with a DCSU-2 corrected spectra unit. Absorption measurements were made on a Beckman DU-8 spectrophotometer.

Nitration of colipase was carried out according to DeCaro *et al.* [6] using procedure III (modification with a low excess of tetranitromethane in the presence of taurodeoxycholate). Purification of the various nitrotyrosyl colipase derivations was accomplished as specified above. The amount of nitrotyrosine was determined by measuring the absorbance ($\epsilon_{381} = 2200\ M^{-1}\cdot cm^{-1}$) and calculation from amino acid compositions. Protein concentration of modified derivatives was determined from amino acid analyses. Sodium dithionite ($Na_2S_2O_4$) reduction of nitrotyrosyl colipase and subsequent dansylation was carried out according to the procedures of Cardin *et al.* [25].

The amount of dansyl-NH-tyrosine present was calculated spectrophotometrically ($\epsilon_{350} = 3980\ M^{-1}\cdot cm^{-1}$ [25]).

Colipase/lipase activity measurements were carried out with tributyrylglycerol emulsions in the presence of 4 mM-taurodeoxycholate at pH 7.5 [24].

C.d. measurements were made with a Cary 61 spectropolarimeter. Standardization of the instrument was accomplished by using a 1 mg/ml aqueous solution of D-10-camphorsulphonic acid as specified by Varian Associates.

Nitropeptide purification was accomplished by using DE-32 cellulose as described by DeCaro *et al.* [6] and by using a Waters h.p.l.c. system with a $C_{18}$ column and propan-1-ol gradient elution (buffer 0.1% trifluoroacetic acid in water).

### Quenching

When quenching occurs by the collisional interaction of a fluorophore (F) and quencher (Q), the change in fluorescence is related to the concentration of quencher by the Stern–Volmer equation [26]:

$$\frac{I_0}{I} = 1 + K_{SV}[Q] = \frac{\tau_0}{\tau} - 1 = k_q\tau_0[Q] \qquad (1)$$

where $I_0$, $\tau_0$ and $I$, $\tau$ are the fluorescence intensities and lifetimes in the absence and presence of Q, respectively, and $K_{SV}$ is the Stern–Volmer quenching constant. The equality of $I_0/I$ with $\tau_0/\tau$ is often used as evidence of a dynamic quenching mechanism. In solvents of low viscosity, where dynamic quenching predominates, the slope of a plot of $I_0/I$ versus [Q] provides a value of the bimolecular rate constant, $k_q$, which is approximated by:

$$k_q = \frac{4\pi N}{1000} q(R_F + D_Q)(D_F + D_Q) \qquad (2)$$

where $N$ = Avogadro's number, $q$ = probability of a collision resulting in quenching, and $R_F$ and $R_Q$ are the radii and $D_F$ and $D_Q$ are the diffusion coefficients of the fluorophore and quencher, respectively.

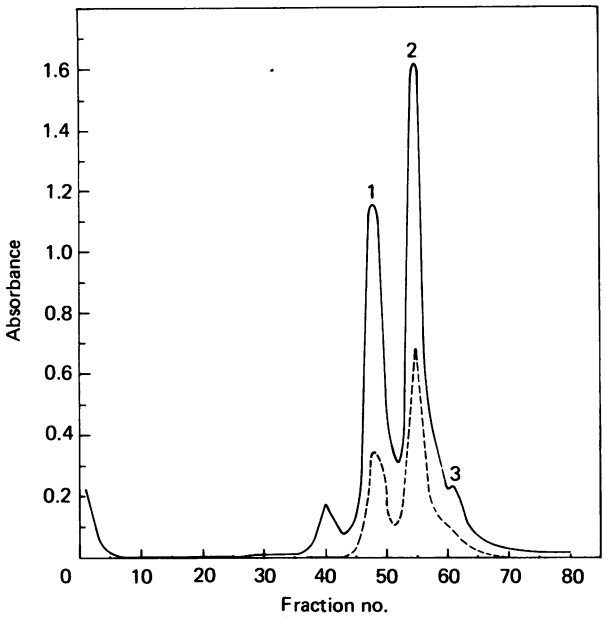


**Fig. 1. Separation of the monomeric nitrated species of porcine colipase on a DEAE-cellulose column (0.9 cm × 20 cm) at 4 °C**

The column was equilibrated with buffer 2[6] and eluted with a linear NaCl gradient (100 ml each, 0–0.25 M) in buffer 2. Flow rate, 3 ml/h; fraction volume, 1.2 ml. ——, $A_{280}$; – – – –, $A_{381}$. Peak 1 contains colipase with a single tyrosine nitrated; peaks 2 and 3 contain colipase in which two and three tyrosines are nitrated, respectively [6].

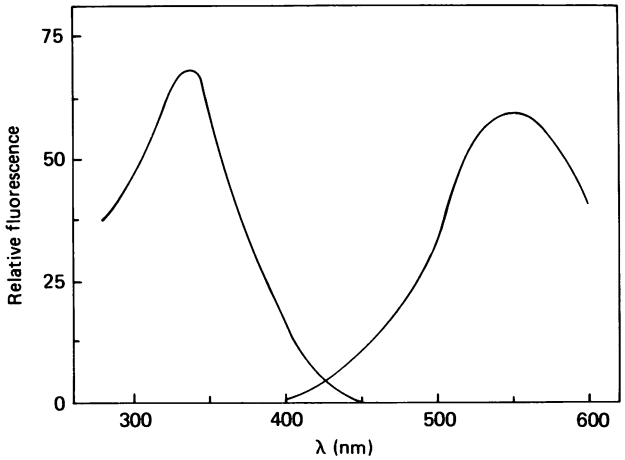


**Fig. 2. Excitation–emission spectra of 5.3 μM monodansyl porcine colipase in 10 mM-Tris/HCl/0.9% NaCl, pH 7.4, 25 °C**

The excitation spectrum (left) was observed at an emission wavelength of 550 nm. The emission spectrum (right) was obtained with an excitation wavelength of 332 nm. The slit widths were both set at 8 nm, and the corrected spectra were run in the ratio mode.

An alternative quenching mechanism referred to as static quenching, has accounted for the upward curvature of some Stern–Volmer plots, especially when the solvent viscosity is increased. Instantaneous quenching will occur when a quencher molecule is within a volume element of the fluorophore at the moment of excitation. The change in fluorescence intensity is given by [26]:

$$\frac{I_0}{I} = e^{V[Q]} \quad (3)$$

where $V$ is the static quenching constant. Plots of $\ln(I_0/I)$ versus [Q] will provide a value of $V$, a parameter independent of solvent viscosity and fluorescence lifetime.

The radius of the volume element referred to above is related to $V$ by the approximation:

$$R \simeq (400\ V)^{\frac{1}{3}} \quad (4)$$

When both static and dynamic quenching are present, the change in fluorescence is described by eqn. (5):

$$\frac{I_0}{Ie^{V[Q]}} - 1 = K_{SV}[Q] \quad (5)$$

$R_{Trp}$, the relative quantum yield of the tryptophanyl residue in horse colipase compared with that of *N*-acetyltryptophanamide, was calculated according to the expression $(F_1/F_2) \times (A_2/A_1)$, where $F_1$ and $F_2$ are the areas under the emission spectra for colipase and *N*-acetyltryptophanamide, respectively, and $A_2$ and $A_1$ are the absorbances at the excitation wavelength for *N*-acetyltryptophanamide and colipase, respectively [27].

The analogous relationship for tyrosine is used to determine $R_{Tyr}$. Areas were determined with the 'Menu' program for the Magiscan Computer (Joyce–Loebel).

The efficiency of energy transfer, $e$, is estimated from the following expression [27]:

$$\varsigma_{Trp(280)}(R_{Trp(280)} - R_{Trp(295)}) = e\varsigma_{Tyr(280)}\ R_{Trp(295)}$$

where $\varsigma$ = fractional absorbance.

Inner filter effects due to the protein and to acrylamide in quenching experiments were corrected by the formula [28]:

$$F_c = F\{\text{antilog}[(A_{ex.} + A_{em.})/2]\}$$

where $F_c$ is the corrected fluorescence intensity, $F$ is the measured intensity, $A_{ex.}$ is the absorbance of the solution at $\lambda_{excitation}$ and $A_{em.}$ is the absorbance of the sample at $\lambda_{emission}$.

## RESULTS

Using our own source of porcine pancreatic acetone powder, nitrated colipase was prepared as described above. The nitrated protein was separated from polymeric species on a Sephadex G-50 column and further purified on a DEAE anion-exchange column. The elution profile of the latter is presented in Fig. 1. The nitrated material from peak 1 was found to contain 1.0±0.1 nitrotyrosine residue/colipase molecule (spectrophotometric and amino acid analysis). Digestion and peptide isolation (DE-32 and h.p.l.c.) confirmed that Tyr-55 had been modified. Activity measurements showed no loss in the ability of the colipase–lipase complex to hydrolyse tributyrylglycerol, and c.d. measurements showed the expected spectral properties as presented by DeCaro *et al.* [6].

Reduction with a 16-fold molar excess of dithionite followed by dansylation with a 5-fold molar excess of dansyl chloride (pH 4.7, 1 h) in the dark at 25 °C resulted in the generation of 1.05±0.1 dansyl-NH-

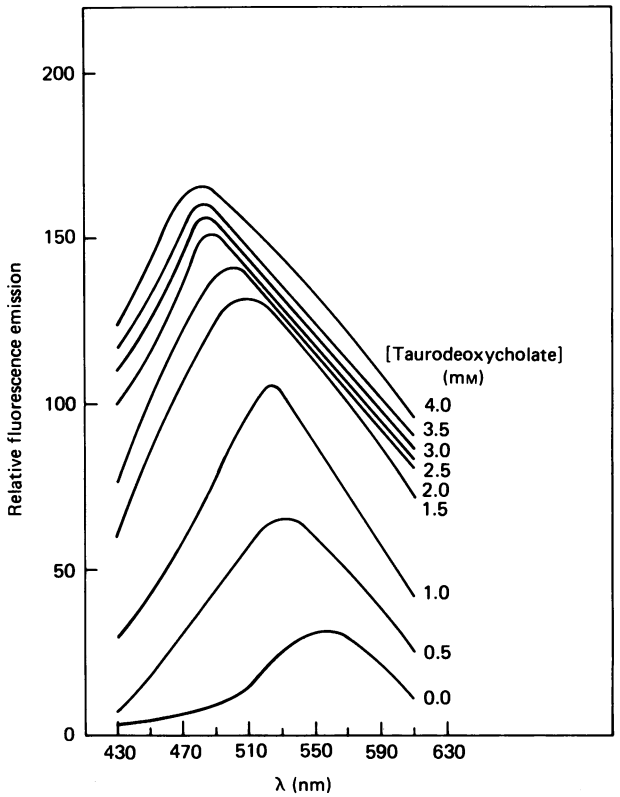


**Fig. 3. Wavelength shifts and quantum yield increases in the emission spectrum for 5.3 μM monodansyl porcine colipase titrated with taurodeoxycholate (0.10 M stock solution)**

The instrument settings and conditions were identical to those in Fig. 2. The lowest curve corresponds to the emission spectrum of dansyl colipase with no addition of taurodeoxycholate. Additions result in final taurodeoxycholate concentrations ranging from 0.5 to 4.0 mM as shown.

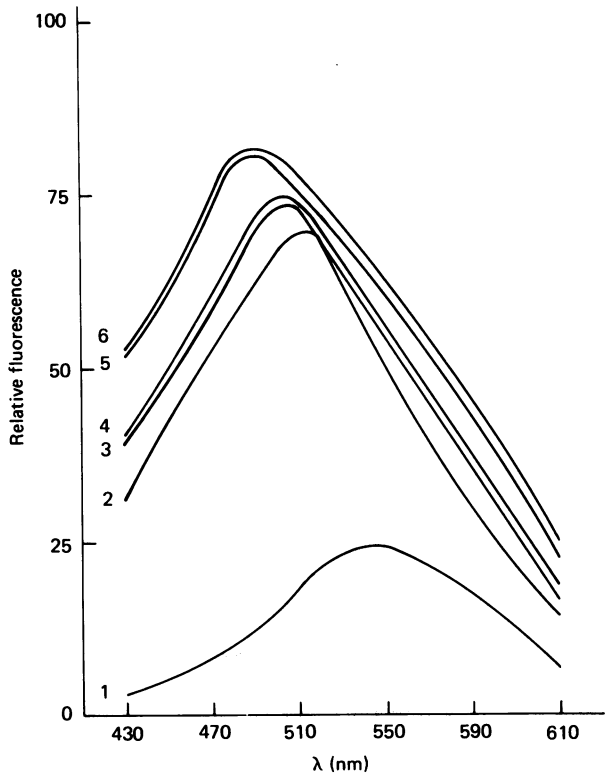


**Fig. 4. Mixed micelle interaction with monodansyl porcine colipase using changes in the emission spectra**

Conditions as previously specified in Figs. 2 and 3. Curve 1, no additions; curves 2–6 are all 10.0 mM in taurodeoxycholate: [taurodeoxycholate]/[oleate] for curve 2 = 2:1, for curve 3 = 10:1, curve 4 = 25:1, curve 5 = 50:1; curve 6 is recorded in the absence of oleate.

tyrosine residues per molecule of colipase. Activity measurements indicated a 2.1-fold increase in colipase-stimulated lipase activity for this new derivative. The emission and excitation spectra of [dansyl-tyr$^{55}$]colipase are presented in Fig. 2. The corrected excitation spectrum is characterized by a maximum at 335 nm while the corrected emission spectrum (excitation at 350 nm) shows a broad maximum centered at 550 nm. Addition of taurodeoxycholate (Fig. 3) causes a marked increase in band intensity (4.3-fold) and a very substantial blue shift to 480 nm. The effect of a mixed micelle system of taurodeoxycholate and oleic acid is shown in Fig. 4. These curves represent a constant [taurodeoxycholate] and are generated by varying the ratio [taurodeoxycholate]/[oleic acid]. Very little effect occurs until the ratio approaches 25:1, and the apparent result is to reduce both the induced amplitude change by taurodeoxycholate and the extent of the blue shift. A Scatchard plot [31] of the fluorescence change induced by taurodeoxycholate is shown in Fig. 5, the data having been taken from a $1/F$ versus 1/[micelle] plot shown in the insert. The plot is linear with $K_d = 6.85 \times 10^{-4}$ M and an intercept value which corresponds to a single micelle (assuming 20 monomers of taurodeoxycholate/micelle

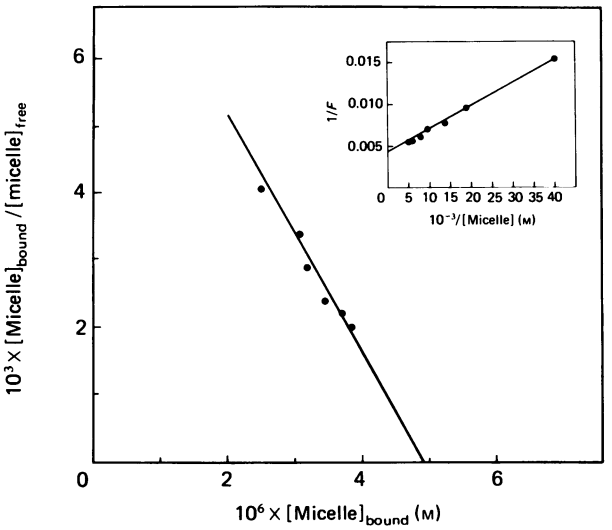


**Fig. 5. Scatchard analysis [31] of the binding of taurodeoxycholate micelles to monodansyl porcine colipase**

The data are taken directly from the maxima positions at various [taurodeoxycholate] from Fig. 3. The inset is a double-reciprocal plot of 1/fluorescence versus 1/[micelle], assuming 20 taurodeoxycholate monomers per micelle [29,30]. The data fit exactly an assumption of one micelle binding site per colipase molecule which is in accord with other binding data using different techniques [29,30]. The analysis indicated a $K_d = 6.85 \times 10^{-4}$ M.

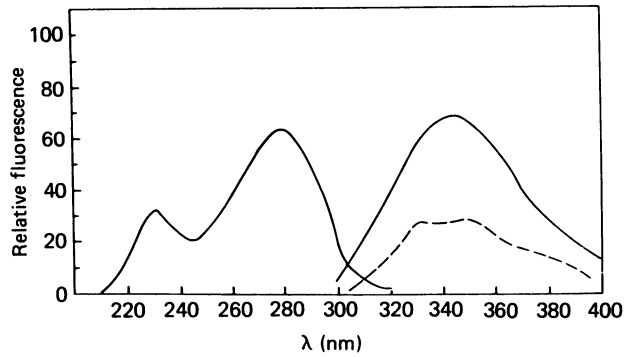


**Fig. 6. Excitation–emission spectra of 2.5 mM equine colipase in 0.05 M-potassium phosphate, pH 7.4, at 25 °C.**

The excitation spectrum (left) was monitored at an emission of 350 nm. Emission spectra (right) are run with excitation wavelengths of 280 nm (——) and 295 nm (– – –). Instrument settings were the same for all three spectra: ratio mode; slit widths 6 nm (excitation) and 8 nm (emission).

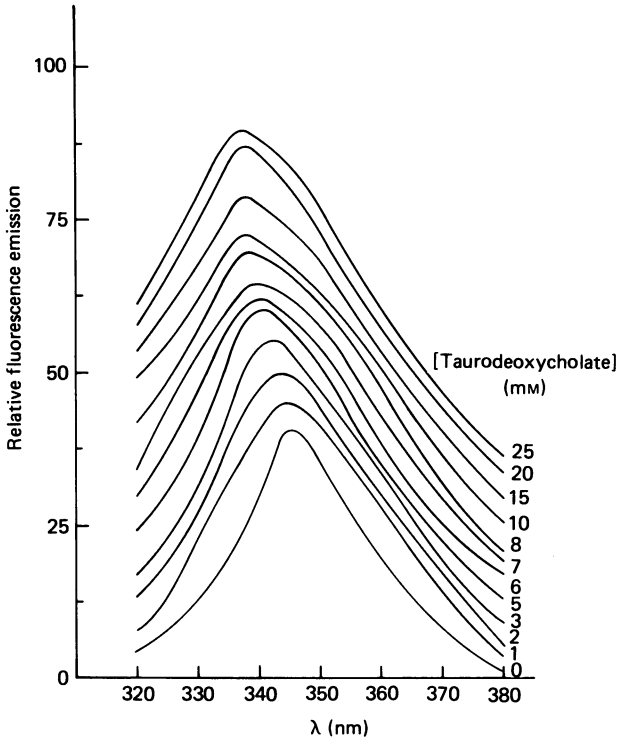


**Fig. 7. Wavelength shifts and quantum yield increases of the emission spectrum for the titration of 2.5 μM horse colipase in 0.05 M-potassium phosphate, pH 7.4, with portions of 0.10 M-taurodeoxycholate in the same buffer**

Excitation wavelength 280 nm; instrument settings are the same as in Fig. 6.

[29, 30]) binding site on colipase as measured by this probe system.

The corrected emission and excitation spectrum of horse colipase is presented in Fig. 6. The latter displayed a broad peak centred at approx. 280 nm, with a small shoulder appearing at 232 nm (emission observation wavelength 350 nm). The emission spectrum was recorded

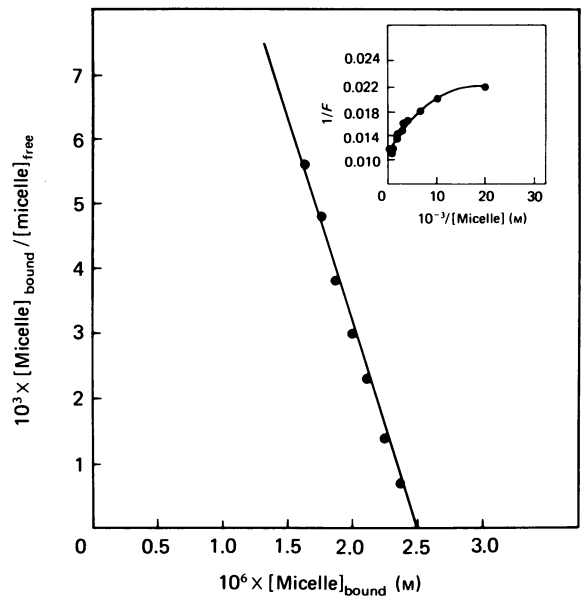


**Fig. 8. Scatchard analysis of the titration of equine colipase with taurodeoxycholate using the maxima positions of the curves shown in Fig. 7**

The inset is a double-reciprocal plot of 1/fluorescence versus 1/[micelle] assuming 20 taurodeoxycholate monomers/micelle [29,30]. Extrapolation to infinite [micelle] provides a value of the limiting fluorescence increase. Only the linear section of this plot was used to construct the Scatchard plot itself. Earlier curvature in the double reciprocal plot (at low [taurodeoxycholate]) is presumed due to dissociation of the micelle below the critical micelle concentration. A value of $K_d = 1.5 \times 10^{-4}$ M was determined from the slope. The intercept indicated a 1:1 relationship between the micelle concentration and that of colipase. If other sites of taurodeoxycholate micelle binding are in fact present, they are not detected by this probe system. Radiolabelled taurodeoxycholate and dialysis experiments support the conclusion of a single micelle binding site [29,30].

at two different excitation wavelengths, 280 and 295 nm. Excitation at 280 nm in order to excite both tyrosine and tryptophan generated a spectrum which is characterized by a broad maximum at 345 nm and a bandwidth at half-height of 57 nm. Excitation at 295 nm generated a bifurcated emission spectrum with $\lambda_{max.}$ at 332 and 350 nm and a double band width of 59 nm. The most pronounced change is a 27% decrease in the relative quantum yield.

### Effect of taurodeoxycholate on the fluorescence emission spectra of horse colipase

The addition of taurodeoxycholate (Fig. 7) to horse colipase near its critical micelle concentration (1 mM [30]) shifts the emission spectrum to the blue from 345 to 337 nm and increases the amplitude (and therefore the quantum yield) of the band nearly 2-fold (1.92). These and similar data allow for the calculation of a binding constant for taurodeoxycholate as well as the number of protein sites involved by using a Scatchard analysis [31]. Fig. 8 shows the data plotted as the concentration of micelle bound divided by the free concentration versus the bound concentration. The insert allows for calcu-

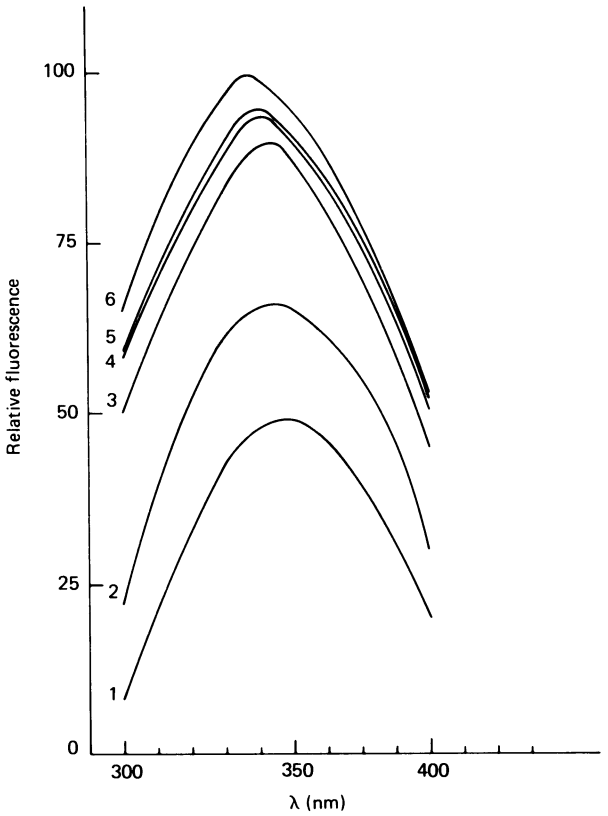


**Fig. 9. Titration of equine colipase with mixed micelles of taurodeoxycholate and oleate by monitoring tryptophan emission**

Curve 1 is generated in the absence of either taurodeoxycholate or oleate. Curves 2–6 are all determined in the presence of 15 mM-taurodeoxycholate with [taurodeoxycholate]/[oleate] ratios which vary as follows: Curve 2, 2:1; curve 3, 10:1; curve 4, 25:1; curve 5, 50:1; curve 6 was determined in the presence of taurodeoxycholate only. Conditions as in Fig. 7.

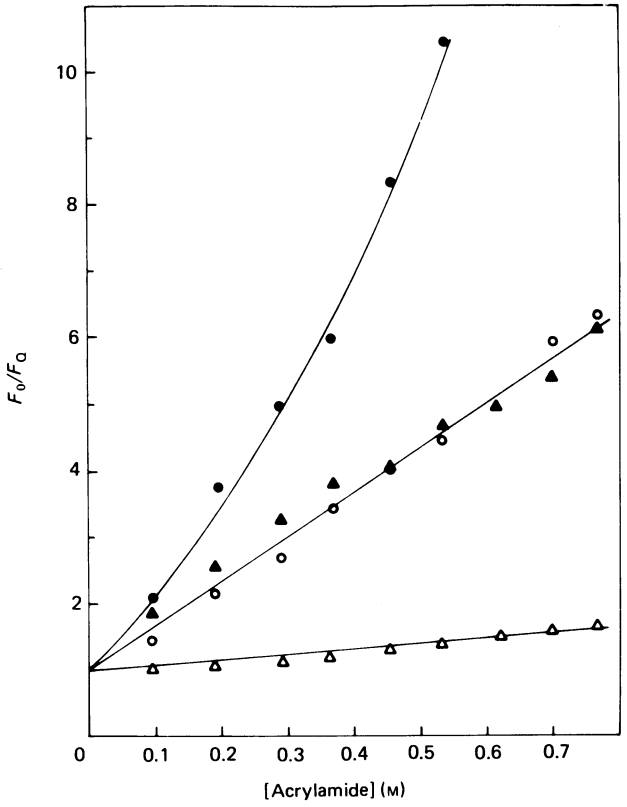


**Fig. 10. Stern–Volmer plot for the quenching of 2.5 μM·equine colipase and 2.5 μM-*N*-acetyltryptophanamide with acrylamide**

Small portions of 5.0 M-acrylamide were added to the solution until a final concentration of 0.725 M quencher was reached. The same titration was performed with water to determine the dilution factor. ●, *N*-acetyltryptophanamide, pH 7.4; ▲, colipase, pH 3.0; ○, colipase, pH 7.4; △, colipase, 94% saturated with taurodeoxycholate, pH 7.4.

lation of the limiting fluorescence change at infinite micelle concentration, using a double reciprocal plot. The data indicate a single micelle binding site on colipase ($n = 1.00 \pm 0.05$) with a $K_d = 1.50 \pm 0.05 \times 10^{-4}$ M (assuming 20 monomeric taurodeoxycholate units/micelle [29,30]). A mixed micelle system was tested here, as for the dansylated porcine colipase (Fig. 9). In this case the effects were larger but still in the same direction, e.g. a diminution of the emission maximum induced by taurodeoxycholate and a reversal of the blue shift.

Table 1 lists some fluorescence parameters for horse colipase and colipase plus taurodeoxycholate and compares these with the same parameters for *N*-acetyltyrosinamide and *N*-acetyltryptophanamide. The relative quantum yield of Trp-52 of colipase is dependent upon $\lambda_{excitation}$ and is an energy acceptor for tyrosine with an $e = 0.27$. The horse colipase–taurodeoxycholate complex showed a 30% quantum yield increase as compared with the uncomplexed protein, but the efficiency of energy transfer dropped to a value of 0.05.

**Table 1. Fluorescence characteristics of horse colipase with and without taurodeoxycholate**

$R_{Tyr}$ is the relative quantum yield of tyrosine in horse colipase as compared with free tyrosine; $R_{Trp}$ is the analogous relationship for tryptophan; $e$ is the efficiency of tyrosine-to-tryptophan energy transfer within horse colipase.

| | $\lambda_{max.(285)}$ (nm) | $\lambda_{max.(295)}$ (nm) | $R_{Tyr(280)}$ | $R_{Trp(280)}$ | $R_{Trp(295)}$ | $e$ |
|---|---|---|---|---|---|---|
| Horse colipase | 345 | 345 | 2.33±0.10 | 0.33±0.03 | 0.26±0.02 | 0.27±0.02 |
| Horse colipase (94% saturated with 25 mM-taurodeoxycholate) | 337 | 340 | 2.78±0.15 | 0.39±0.03 | 0.37±0.02 | 0.05±0.01 |

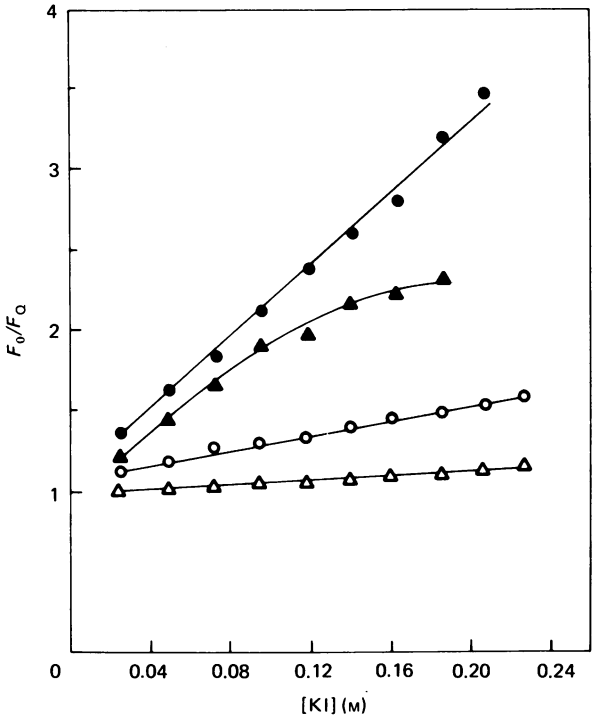


**Fig. 11. Stern–Volmer plot for the quenching of equine colipase and *N*-acetyltryptophanamide with KI**

Small portions of 2.5 M-KI were added to the solution until a final concentration of 0.23 M quencher was reached. The dilution factor was calculated by doing the same titration with 2.5 M-NaCl. ●, *N*-acetyltryptophanamide, pH 7.4; ▲, colipase, pH 3.0; ○, colipase, pH 7.4; △, colipase, 94% saturated with taurodeoxycholate, pH 7.4.

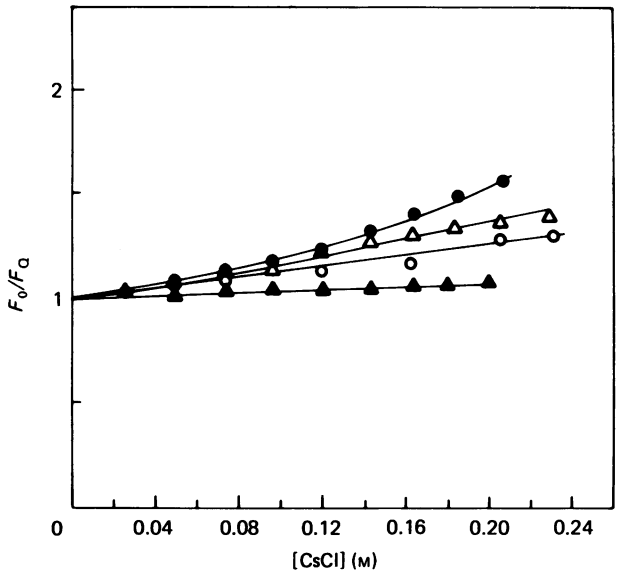


**Fig. 12. Stern–Volmer plot for the quenching of equine colipase and *N*-acetyltryptophanamide with CsCl**

Small portions of 2.5 M-CsCl were added to the solution until a final concentration of 0.23 M quencher was reached. Dilution factor was calculated by titrating the protein solution with 2.5 M-NaCl. ●, *N*-acetyltryptophanamide, pH 7.4; △, colipase, pH 7.4; ○, colipase, pH 3.0; ▲, colipase, 94% saturated with taurodeoxycholate, pH 7.4.

The relative quantum yield values for tyrosine were high in both cases.

### Quenching experiments

The fluorescence quenchers acrylamide, $I^-$, and $Cs^+$ were used to probe the environment of Trp-52 of colipase. The Stern–Volmer plots for each (Figs. 10, 11, and 12) yielded the $K_{SV}$ values shown in Table 2. The interaction of each of these ions with colipase was investigated both in the presence and absence of taurodeoxycholate and the $K_{SV}$ values ($M^{-1}$) were compared with those of *N*-acetyltryptophanamide. Acrylamide quenching of colipase yielded a $K_{SV}$ value of 7.00 compared with 14.50 for *N*-acetyltryptophanamide. Lowering the pH value to 3.0 had no effect on this value. Iodide quenching, on the other hand, was less efficient at pH 7.4 compared with acrylamide, but lowering the pH to 3.0 increased the quenching to a value even higher than for acrylamide. Caesium acted oppositely to iodide, in that its quenching efficiency was higher at pH 7.4 than at 3.0. At 94% saturation of colipase with taurodeoxycholate, the efficiency of $I^-$ and acrylamide quenching drops dramatically to a value of approx. 5%, while that of caesium falls to 20%.

**Table 2. Fluorescence quenching studies on colipase**

($K_{SV}$) values for lines with upward curvature were calculated by averaging the slopes of the tangents to each point of the Stern–Volmer plot. This applied only to the quenching of model compounds for which there was a relatively small static quenching component.

| | $K_{SV}$ ($M^{-1}$) | | |
|---|---|---|---|
| Quencher . . . | $Cs^+$ | $I^-$ | Acrylamide |
| *N*-Acetyltryptophanamide | 2.25±0.25 | 12.00±1.00 | 14.50±1.50 |
| Horse colipase (pH 7.4) | 1.65±0.25 | 3.33±0.50 | 7.00±0.50 |
| Horse colipase (pH 3.0) | 1.15±0.15 | 8.50±1.0 | 7.00±0.50 |
| Horse colipase (+taurodeoxycholate) | 0.46±0.09 | 0.63±0.10 | 0.65±0.10 |

## DISCUSSION

Reduction and dansylation of [nitrotyrosine-55] colipase yields a new fluorescent derivative of porcine pancreatic colipase that is coenzymically 210% active compared with native colipase in a normal lipase assay with tributyrylglycerol. Substitution in colipase with such a relatively bulky group would seem to suggest at first glance that Tyr-55 could not play a major role in colipase activation of lipase. However, the steric restrictions imposed in this system are not known as there are few precedents for these kinds of interactions, and certainly classic lock and key substrate specificity is not a suitable model.

In so far as taurodeoxycholate mimics or serves as a paradigm of lipase–colipase–interface activity, dansyl-colipase responds dramatically to this addition. The emission band intensity increases 4.3-fold and the blue shift is a full 70 nm. Increases in intensity and blue shifts are generally indicative of a movement to a more hydrophobic environment for the [dansyl-NH-Tyr$^{55}$]-colipase probe and may in fact indicate actual insertion of the modified residue into the hydrophobic interior of the micelle. The Scatchard plot of the data shows a dissociation constant that is in agreement with other studies of this interaction [24,29,30,32], and further indicates a clear one-to-one micelle interaction and establishes this as a valid probe system. The effects of mixed micelles in this system and in the horse system are minimal until the lower ratios of [taurodeoxycholate]/[oleic acid] are reached and the effect noticed is an apparent disruption of the interaction in both cases and therefore would be consistent with a bulk effect on the micelles themselves.

It is interesting to compare these spectral results with those of Meyer *et al.* [19] for the phospholipase $A_2$ system. Taurodeoxycholate micelles have virtually no effect on the spectral properties of free dansyl-NH-tyrosine (J. C. McIntyre, unpublished work); this is in marked contrast with the effects of *n*-hexadecylphosphocholine (the micelle in the phospholipase $A_2$ system) on *N*-acetyl-3-dansylaminotyrosine ethyl ester or dansyltryptophan. The largest spectral effects of hexadecylphosphocholine on the enzyme system are those on horse [dansyl-NH-Tyr$^{19}$]phospholipase $A_2$ in which there is a 400% amplitude increase. This is comparable with that of [dansyl-NH-Tyr$^{55}$] colipase by taurodeoxycholate in which there is a 430% band amplitude increase. The spectral blue shift induced on dansyl-colipase by taurodeoxycholate, however, is nearly three times that reported for dansyl-phospholipase $A_2$ [19]. In the latter system, the introduction of an apolar dansyl side chain on both aminotyrosine-69 and aminotyrosine-19 actually improves the affinity of the enzyme for lipid–water interfaces, and in our system the activity of dansyl-colipase actually doubles. This improved affinity indicated to Meyer *et al.* [19] that both residues, in particular Tyr-19, are directly involved in the hydrophobic interaction with the apolar fatty acid chain and may in fact move into the micelle completely. Our results are quite compatible with this interpretation.

Colipase surface interaction may be quite similar to the interface recognition site of the phospholipases. As has been pointed out [19], this site is not equivalent to a substrate binding site and therefore may be correspondingly less stringent in binding modified residues, particularly modified tyrosine. In recent X-ray structural analysis of the bovine phospholipase system, Tyr-69 and Leu-19 (which is a tyrosine residue in the horse enzyme [21]) are both implicated as forming part of the interface recognition site and doubtless the leucine will function in a hydrophobic binding capacity. In view of the striking similarities of the dansyl-colipase and phospholipase $A_2$ systems, the latter of which enjoys X-ray crystallographic conformation of tyrosyl residue interaction, it is concluded that Tyr-55 does indeed participate in micelle interaction in native colipase. The role of the second tyrosine residue modified by tetranitromethane (Tyr-59), which generates considerable optical activity and response to taurodeoxycholate [6], needs further investigation.

The presence of a single residue of tryptophan in horse colipase provides an excellent system for protein fluorescence studies. The emission maximum at 345 nm indicates a relatively solvent-accessible tryptophan residue in equine colipase. The $\lambda_{max.}$ value for a deeply buried residue would approach 308 nm, as found in azurin [33], compared with 352 nm for the exposed tryptophans in glucagon and adenocorticotropin [33]. The $K_{SV}$ value for acrylamide quenching of Trp-52 of colipase is 7.0 $M^{-1}$, which falls between $K_{SV}$ values for glucagon and human growth hormone (10.5 and 3.0 $M^{-1}$, respectively). This is in marked contrast to azurin, which exhibits a $K_{SV}$ value of approx. 0.

The dependence of the emission intensity on the excitation wavelength is indicative of tyrosine–tryptophan energy transfer. In the case of colipase, there is a 60% drop in intensity upon excitation at 295 nm, which would be specific for tryptophan excitation. The excitation band at 232 nm could possibly be due to phenylalanine residues in colipase.

Titration of colipase with taurodeoxycholate in the range of its critical micelle concentration causes a blue-shift of 8 nm, which is indicative of a more hydrophobic environment for tryptophan. This could be the consequence of either an induced change in protein conformation or a result of direct binding of taurodeoxycholate to the tryptophan residue. Such shifts do occur in micelle binding of indole [23] as well as an apparent decrease in $K_{SV}$ for acrylamide quenching, both of which are occurring here. Double reciprocal plots of $1/F$ versus $1/[(\text{taurodeoxycholate})_{20}]$ (20 monomers/micelle is correct for the ionic strength used in these experiments [30]) allow extrapolation of the fluorescence value at infinite micelle concentration. A Scatchard plot of the data yields a linear plot whose intercept corresponds to a single micelle binding site with a $K_d$ fully consistent with previous data [29,30,32]. An absence of curvature indicates a lack of co-operativity, and a single intercept indicates a unique binding site, and the absence of multiple weak interactions.

The results of the quenching experiments support the conclusion that taurodeoxycholate reduces the accessibility of the tryptophan residue in colipase. Whether this is accomplished by direct steric or charge interactions, or by induced conformational interactions, cannot be determined by the experiments reported here. The lowering of pH from 7.4 to 3.0 (colipase is quite stable at pH 3.0) had little effect on acrylamide quenching, as might be anticipated due to its lack of formal charge. The rather dramatic effect of pH on iodide quenching would suggest the presence of a negatively charged residue(s) in the vicinity of Trp-52. The relatively smaller

decrease in accessibility of tryptophan in the presence of taurodeoxycholate by caesium ions may be due to its smaller size or possibly some electrostatic interactions with the taurine moiety of taurodeoxycholate. Taken together, the data support a role of tryptophan in taurodeoxycholate binding in equine colipase, though a role for tyrosine is also likely by analogy with the porcine system. The fact that a lysyl residue is present in human colipase at position 52 suggests that further study of the latter system must be carried out to see if there are kinetic and thermodynamic differences between them. If there are not, then induced conformational effects translated to the environment of tryptophan in horse colipase may be the preferred mechanistic explanation. The participation of direct aromatic side chain residues in the porcine system seems highly probable.

The authors acknowledge grant support (HL-30431) from the National Institutes of Health.

## REFERENCES

1. Sémériva, M. & Desnuelle, P. (1976) Horiz. Biochem. Biophys. **2**, 32–39
2. Borgström, B., Erlanson-Albertsson, C. & Wieloch, T. (1979) J. Lipid Res. **20**, 805–816
3. Sémériva, M. & Desnuelle, P. (1979) Adv. Enzymol. **48**, 319–370
4. Charles, M., Sémériva, M. & Chabre, M. (1980) J. Mol. Biol. **139**, 297–317
5. Behnke, W. D. (1982) Biochim. Biophys. Acta **708**, 118–123
6. DeCaro, J. D., Behnke, W. D., Bonicel, J. J., Desnuelle, P. A. & Rovery, M. (1983) Biochim. Biophys. Acta **747**, 253–262
7. Charles, M., Erlanson, C., Bianchetta, J., Joffre, J., Guidoni, A. & Robery, M. (1974) Biochim. Biophys. Acta **359**, 186–197
8. Bonicel, J., Couchoud, P., Foglizzo, E., Desnuelle, P. & Chapus, C. (1981) Biochim. Biophys. Acta **669**, 39–45
9. Canioni, P. & Cozzone, P. (1979) Biochimie **61**, 343–354
10. Wieloch, T., Borgström, B., Falk, K. E. & Forsen, S. (1979) Biochemistry **18**, 1622–1628
11. Canioni, P., Cozzone, P. & Sarda, L. (1980) Biochim. Biophys. Acta **621**, 29–42
12. Canioni, P., Cozzone, P. & Kaptein, R. (1980) FEBS Lett. **111**, 219–222
13. Cozzone, P., Canioni, P., Sarda, L. & Kaptein, R. (1981) Eur. J. Biochem. **114**, 119–126
14. Sari, H., Entressangles, B. & Desnuelle, P. (1975) Eur. J. Biochem. **58**, 561–65
15. Charles, M., Sari, H., Entressangles, B. & Desnuelle, P. (1975) Biochem. Biophys. Res. Commun. **65**, 740–745
16. Sauve, P. & Desnuelle, P. (1980) FEBS Lett. **122**, 91–94
17. Sari, H., Granon, S. & Sémériva, M. (1978) FEBS Lett. **95**, 229–234
18. Jansen, E. H. J. M., Meyer, H., De Haas, G. H. & Kaptein, R. (1978) J. Biol. Chem. **253**, 6346–6347
19. Meyer, H., Puijk, W. C., Dijkman, R., Foda-Van der Hoorn, M. M. E. L., Pattus, F., Slotboom, A. J. & DeHaas, G. H. (1979) Biochemistry **18**, 3589–3597
20. Dijkstra, B. W., Kalk, K. H., Hol, W. G. J. & Drenth, J. (1981) J. Mol. Biol. **147**, 97–123
21. Djikstra, B. W., Drenth, J. & Kalk, K. H. (1981) Nature (London) **289**, 604–606
22. Erlanson, C., Barrowman, J. & Borgström, B. (1977) Biochim. Biophys. Acta **489**, 150–162
23. Sternby, B., Engstrom, A., Hellman, U., Vihert, A. M., Sternby, N. & Borgström, B. (1984) Biochim. Biophys. Acta **784**, 75–80
24. Chapus, C., Desnuelle, P. & Foglizzo, E. (1981) Eur. J. Biochem. **115**, 99–105
25. Cardin, A. D., Jackson, R. L. & Johnson, J. D. (1982) J. Biol. Chem. **257**, 4987–4992
26. Blatt, E. & Sawyer, W. H. (1985) Biochim. Biophys. Acta **822**, 43–62
27. Kahan, I., Epand, R. M. & Moscarello, M. A. (1986) Biochemistry **25**, 562–566
28. Hill, B. C., Horowitz, P. M. & Robinson, N. C. (1986) Biochemistry **25**, 2287–2292
29. Charles, M., Astier, M., Sauve, P. & Desnuelle, P. (1975) Eur. J. Biochem. **58**, 555–559
30. Sari, H., Entressangles, B. & Desnuelle, P. (1975) Eur. J. Biochem. **58**, 561–565
31. Scatchard, G. (1949) Ann. N.Y. Acad. Sci. **51**, 660–672
32. Canioni, P., Julien, R., Romanetti, R., Cozzone, P. & Sarda, L. (1981) Biochim. Biophys. Acta **670**, 305–311
33. Eftink, M. R. & Ghiron, C. A. (1976) Biochemistry **15**, 672–680

Received 15 October 1986/12 March 1987; accepted 15 April 1987